BULLETIN
OF THE KOREAN CHEMICAL SOCIETY

VOLUME 7, NUMBER 4
AUGUST 20, 1986

BKCS 7(4) 257-330 (1986)
ISSN 0253-2964

# A New Flow Equation for Thixotropic Systems

**Dae-Won Sohn, Eung-Ryul Kim, and Sang-Joon Hahn**

*Department of Chemistry, Hanyang University, Seoul 133*

**Taikyue Ree***

*Department of Chemistry, The Korea Advanced Institute of Science and Technology, Seoul 131*

*Received February 25, 1986*

Thixotropy is a time-dependent shear-thinning phenomenon. We derived a new thixotropic formula which is based on the generalized viscosity formula of Ree and Eyring, $f=\Sigma\frac{X_i}{\alpha_i}\sinh^{-1}(\beta_i\cdot\dot{s})$ (Refer to the text concerning the notation.) The following is postulated: (1) thixotropy occurs when small flow units attached to a large flow unit separate from the latter under stress (2) elastic energy($\omega$) is stored on the large flow unit during the flow process, and (3) the stored energy contributes to decrease the activation energy for flow. A new thixotropic formula was derived by using these postulations, $f=\frac{X_0\beta_0}{\alpha_0}\dot{s}+\frac{X_1\beta_1}{\alpha_1}\dot{s}+\frac{X_2}{\alpha_2}\sinh^{-1}[(\beta_0)_2\exp(-C_2\dot{s}^2/RT)\cdot\dot{s}]$ f is the shear stress, and $\dot{s}$ is the rate of shear. In case of concentrated solutions where the Newtonian flow units have little contribution to the viscosity of the system, the above equation becomes, $f=\frac{X_2}{\alpha_2}\sinh^{-1}[(\beta_0)_2\exp(-c_2\dot{s}^2/RT)\cdot\dot{s}]$ In order to confirm these formulas, we applied to $TiO_2$(anatase and rutile)-water, printing ink and mayonnaise systems. Good agreements between the experiment and theory were observed.

## Introduction

Thixotropiy is a time-dependent shear-thinning phenomenon.[1,2] Since 1923, the gel → sol transition of $Fe_2O_3$ aqueous dispersions[3] and many interesting observations on thixotropy have been reported. Thixotropic studies started from inelastic systems, then developed remarkably since they were connected with viscoelastic systems like polymer solutions.

Thixotropic phenomena appear in various fields such as paint, polymer and food industries.[4] Recently, the thixotropy is found in the fields of biochemistry[5,6] and materials science.[7,8] In spite of the various observations, thixotropic data are too fragmentary for systematic studies. The interrelation between structure and mechanical properties of thixotropic systems are relatively little know.[9] Early attempts to analyze thixotropic behavior were centered on qualitative or empirical concepts obtained from hysteresis-loop measurements.[10]

Thixotropy is defined here as the phenomenon having the following characteristics,[4] (1) it accompanies an isothermal decrease of viscosity with increasing shear rate, (2) a structural change is irreversibly brought about by a mechanical disturbance applied to the system, (3) when the mechanical disturbance is removed, the system recovers its original structure, and (4) the flow curves(shear rate vs. shear stress) of the system show a hysteresis loop,[11] when the concentration of the system is reasonably high. These statements are similar to Bauer and Collins' definition.[3]

There are two main streams in the theoretical interpretations of thixotropic phenomena.[12] One is Goodeave's network theory[13] and the other is the Ree-Eyring's kinetic theory.[4] In 1955, by developing Eyring's theory of transport phenomena,[14] the generalized vicosity formula known as the Ree-Eyring equation was derived.[15] In 1957, Hahn *et al.* applied the generalized viscosity formula to the thixotropic hysteresis.[16]

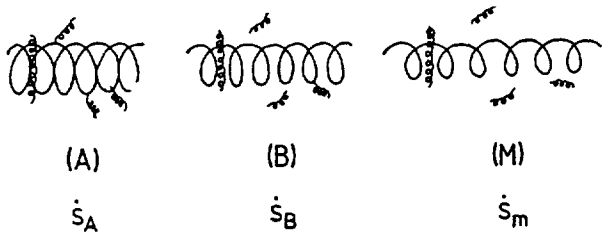


**Figure 1.** The model of a non-Newtonian unit. (A) The state without stress, (B) the state under stress, (M) the state under higher stress.

Many other investigators developed their own theories with the constitutive equations of inelastic viscous fluids.[17-20] Fredrickson[20] proposed the inelastic thixotropic model of viscous fluids, which do not exhibit such as viscoelastic phenomena, recoil or stress relaxation. On the other hand, the kinetic theory[4] has the concept of viscoelasticity which is connected with the strain energy or relaxation time. By developing the kinetic theory further, Park and Ree[21] proposed an elaborate theory which is successfully applied to bentonite suspensions. In 1971, Utsugi and Ree[22] studied the Ostwald curves which is related to thixotropy, and showed that their equation of flow is related with the Einstein equation of flow.[23]

In this paper, by introducing the concept of structural change caused by the shear stress into the Ree-Eyring equation of flow, a modified and simple thixotropic equation is derived. This new thixotropic equation is applied to inelastic and viscoelastic systems, then the parameters of the thixotropic equation are investigated.

## Theory

**1. Model of Thixotropy.** We assume that a non-Newtonian unit has a structure as shown by Figure 1A, *i.e.*, it is a tiny spring in which several short springs are attached. The short springs are tightly attached, and they do not detach if no force is applied to the main spring. Figure 1B shows the state when force applied to the main spring; one notices that the latter is elongated and that some short springs are detached. In Figure 1M is shown the state when stronger force is applied to the main spring, as a result, it is more elongated, and more short springs are detached. The short springs represent the flow units 1. As long as the main-spring is under stress field, the detached small springs do not reattach to the main-spring, *i.e.*, the recovery does not occur. The recovery occurs only when the stress is completely removed. The detachment and reattachment is the model of thixotropy.

Hahn, Ree and Eyring[4] showed that when a molecule is under a stress field which produces strain rate $\dot{s}$, it is deformed and the strain energy $c\dot{s}^2$ ($c$ is constant) is stored in the molecule. In the above mentioned model, the strain energy is proportional to the elongation of the main-springs and to the number of detached small springs.

When no stress is applied to the flow unit (Figure 1A), the activation free-energy for flow $\Delta G_0^*$ is very large since the unit accompanies many small springs with it. But, under a stress(flow) field of $\dot{s}_B$, some of small springs are detached from the unit (Figure 1B), the activation free energy becomes $\Delta G_0^* - c\dot{s}_B^2$, *i.e.*, it decrease. When the stress is more increased (Figure 1M), almost all the small springs are removed from the unit, the flow activation-energy decreases to $\Delta G_0^* - c\dot{s}_m^2$ where $\dot{s}_m > \dot{s}_B$.

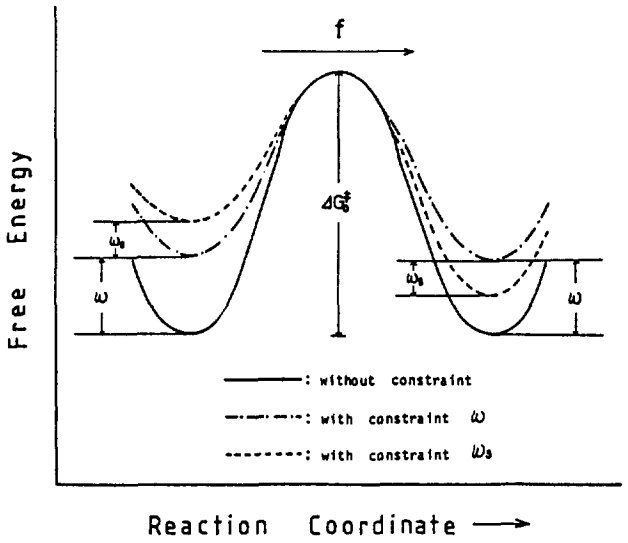


**Figure 2.** The activation free energy curves for flow. The work $\omega_s$ is the constraint causing the flow, and $\omega$ is the strain energy stored on the flow unit which helps the detachment of small flow unit, consequently helping the flow.

**2. Flow Equation.** The activation free-energy diagram for flow of the flow unit is shown in Figure 2, where $\omega = c\dot{s}^2$, $\omega_s = \lambda\lambda_2\lambda_3 fN/2$, $N$ is Avogadro number, $f$ is the shear stress, and $\lambda$, $\lambda_2$, $\lambda_3$ are the molecular dimensions introduced by Eyring.[14] From Figure 2, one knows that

$$\Delta G_f^* = \Delta G_0^* - \omega - \omega_s \text{ and } \Delta G_b^* = \Delta G_0^* - \omega + \omega_s$$

where the subscript $f$ and $b$ indicate the direction of jump of the flow unit, *i.e.*., forward and backward, respectively. The rate constants $k_f$ and $k_b$ are represented, respectively,

$$k_f = (kT/h)\cdot\exp[-(\Delta G_0^* - \omega - \omega_s)/RT] \quad (1)$$

$$k_b = (kT/h)\cdot\exp[-(\Delta G_0^* - \omega + \omega_s)/RT] \quad (2)$$

If the net rate forward is represented by $k'(=k_f - k_b)$ the rate of shear $\dot{s}$ is expressed by[14]

$$\begin{aligned}\dot{s} &= (\lambda/\lambda_1)\cdot k' \\ &= (\lambda/\lambda_1)\cdot(2kT/h)\cdot\exp[-(\Delta G_0^* - \omega)/RT]\cdot\sinh(\omega_s/RT) \\ &= (\lambda/\lambda_1)\cdot 2k_0\cdot\exp(\omega/RT)\cdot\sinh(\omega_s/RT) \\ &= 2(\lambda/\lambda_1)k_0\cdot\exp(c\dot{s}^2/RT)\cdot\sinh(\lambda\lambda_2\lambda_3 f/2kT) \end{aligned} \quad (3)$$

where $k_0$ is the rate constant when there is no stress, *i.e.*,

$$k_0 = (kT/h)\cdot\exp(-\Delta G_0^*/RT) \quad (4)$$

Equation (3) is rewritten as,

$$f = (1/\alpha)\sinh^{-1}[\beta_0\cdot\exp(-c\dot{s}^2/RT)\dot{s}] \quad (5)$$

where

$$\alpha = (\lambda\lambda_2\lambda_3/2kT) \quad (6)$$

and

$$\beta_0 = (2k_0\lambda/\lambda_1)^{-1} \quad (7)$$

The $1/\alpha$ and $\beta$ are the physical properties proportional to the shear modulus and relaxation (when there is no stress), respectively. If there are various kinds of flow units in the flow system, we may express $f$ as[15]

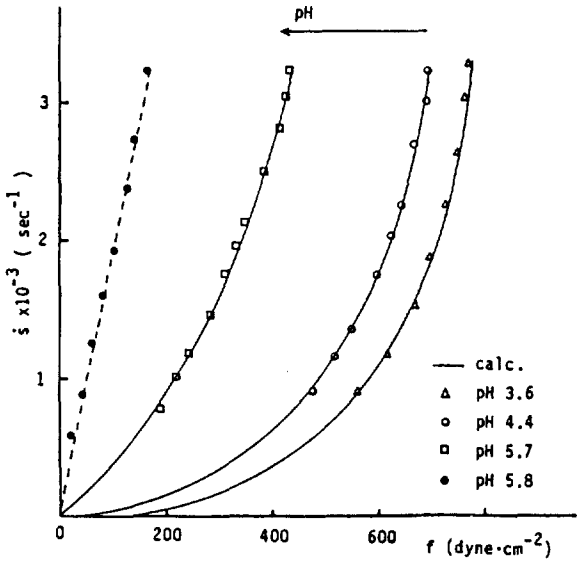


**Figure 3.** Flow curves of 30wt.% $TiO_2$(anatase)-water suspension with various pH at 25°C.

$$f=\Sigma X_i f_i=\Sigma \frac{X_i}{\alpha_i}\sinh^{-1}[(\beta_0)_i\dot{s}\cdot\exp(-c_i\dot{s}^2/RT)] \quad (8)$$

where $X_i$ is the fraction of the area occupied by the $i$-th kind of flow units. In many cases, Eq.(8) is simplified as

$$f=\frac{X_0\beta_0}{\alpha_0}\dot{s}+\frac{X_1\beta_1}{\alpha_1}\dot{s}+\frac{X_2}{\alpha_2}\sinh^{-1}[(\beta_0)_2\dot{s}\cdot\exp(-c_2\dot{s}^2/RT)] \quad (9)$$

The subscript 0 and 1 represent the solvent and unit 1 (both being Newtonian), respectively, $c_i=0$, and $\sinh^{-1}[(\beta_0)_i\dot{s}]=(\beta_0)_i\dot{s}$ where $i=0$ or 1. When the Newtonian terms in Eq.(9) is negligibly small, it becomes,

$$f=\frac{X_2}{\alpha_2}\sinh^{-1}[(\beta_0)_2\cdot\dot{s}\cdot\exp(-c_2\dot{s}^2/RT)] \quad (10)$$

Equation (10) is very similar to Bang *et al.*'s equation for dilatancy[24] except for the sign in the factor $\exp(-c_2\dot{s}^2/RT)$ since it becomes $\exp(c_2\dot{s}^2/RT)$ in Bang *et al.*'s equation.

The flow curves obtained with increasing $\dot{s}$ with time is called the up-curve, Eq.(9) or (10) is applied to the up-curve. The down-curve is the flow curve obtained with the decreasing $\dot{s}$ with time. For the down-curve, the following equation is applied:

$$f=\frac{X_0\beta_0}{\alpha_0}\dot{s}+\frac{X_1\beta_1}{\alpha_1}\dot{s}+\frac{X_2}{\alpha_2}\sinh^{-1}[(\beta_0)_2\cdot\dot{s}\cdot\exp(-c_2\dot{s}_m^2/RT)] \quad (11)$$

where $\dot{s}_m$ is the maximum shear rate(Figure 1M) from which the down-curve starts. The reason is as follows: (1) at the apex, the flow equation is also represented by Eq.(11), and (2) all the parameters in Eq.(11) will not change in the course of the down-curve since no recovery occurrs in this process.

By using the above-mentioned model, which is applicable to any case of thixotropy, the results (see the chapter) were obtained, and the related subjects are discussed.

## Applications

**1. $TiO_2$(anatase)-water Suspension.** The author's theory is applied to the thixotropic system of $TiO_2$(anatase)-water system. Lee *et al.* measured the viscosities of the anatase-water suspension by a Couette-type rotational viscometer.[25] They reported the dilatancy-thixotropy transition occurs at pH=5.8 which is induced by the electrolytes added to the system. It was also reported that the anatase-water suspension presents a dilatant phenomenon above pH=5.8 and a thixotropy below pH=5.8. The flow curves in Figure 3 are those for the pH effect on the flow properties of $TiO_2$(anatase)-water suspension(pH<5.8).

**Table 1. Flow Parameters for $TiO_2$-Water Suspension, Printing Ink and Mayonnaise Systems**

| | | $X_0\beta_0/\alpha_0+X_1\beta_1/\alpha_1$ | $X_2/\alpha_2$ | $(\beta_0)_2$ | $c_2/RT$ |
|---|---|---|---|---|---|
| $TiO_2$(anatase)-water suspension | | | | | |
| | pH 3.6 | | 183.0 | 16.44 | $4.893\times10^{-8}$ |
| | pH 4.4 | | 181.5 | 9.547 | $2.901\times10^{-8}$ |
| | pH 5.7 | | 169.2 | 2.452 | $0.650\times10^{-8}$ |
| $TiO_2$(rutile)-water suspension | | | | | |
| | pH 5.4 | | 62.81 | 0.745 | — |
| | pH 6.3 | | 46.89 | 1.729 | $3.547\times10^{-9}$ |
| | pH 7.1 | | 50.14 | 2.071 | $5.066\times10^{-9}$ |
| Printing Ink | | | | | |
| small($\dot{s}_m=170s^{-1}$) | | 2.417 | 5.928 | 1.124 | $2.957\times10^{-4}$ |
| large($\dot{s}_m=1100s^{-1}$) | | 1.251 | 7.134 | 0.536 | $0.858\times10^{-4}$ |
| Mayonnaise | | | | | |
| ($\dot{s}_m=1450s^{-1}$) | 20°C | 1.159 | 711.9 | 0.138 | $3.918\times10^{-7}$ |
| | 33°C | 1.075 | 433.7 | 0.364 | $4.793\times10^{-7}$ |

$X_0\beta_0/\alpha_0+X_1\beta_1/\alpha_1$: dyne·sec·cm$^{-2}$, $X_2/\alpha_2$: dyne·cm$^{-2}$, $(\beta_0)_2$: sec, $c_2/RT$: sec$^2$.

In Figure 3 only the up-curves are presented, because the down-curves are nearly overlapped with the up-curves, *i.e.*, no hysteresis loop. This shows that the recovery to the original structure is very quick. Eq.(10) was applied to the $TiO_2$ (anatase)-water system, and the parametric values listed in Table 1 were obtained. The theoretical curves were calculated from Eq.(10) by using the parametric values. One notes that the agreement between theory and experiment is very good.

**2. $TiO_2$(rutile)-water Suspension.** The titanium dioxide has three crystal modifications, rutile, anatase and brookite, all of which occur in nature. Their structural difference cause the change of physical properties.

In the case of 30wt.% anatase-water suspension, it has a dilatancy-thixotropy transition at pH=5.8. But for the rutile($TiO_2$)-water suspension the dilatancy-thixotropy transition occurrs at the two points of pH=5.0 and pH=8.8. Rutile system presents the dilatant phenomena below pH=5.0 and above pH=8.8, and the thixotropy between pH=8.8 and pH=5.0. Figure 4 represents the up-curves of 35wt.% rutile-water suspension at various pH at 25°C. In this case also, no hysteresis loop was observed. The parametric values found by applying Eq.(10) are included in Table 1. As we can see from Figure 4, the calculated thixotropic flow curves and the experiments are also in good agreement.

The $TiO_2$ suspension is treated as a special case of thixotropy where no hysteresis loop appears. The reason for the disappearance of the hysteresis loop is as follows: the reattachment of the detached units is very quick, *i.e.*, the recovery

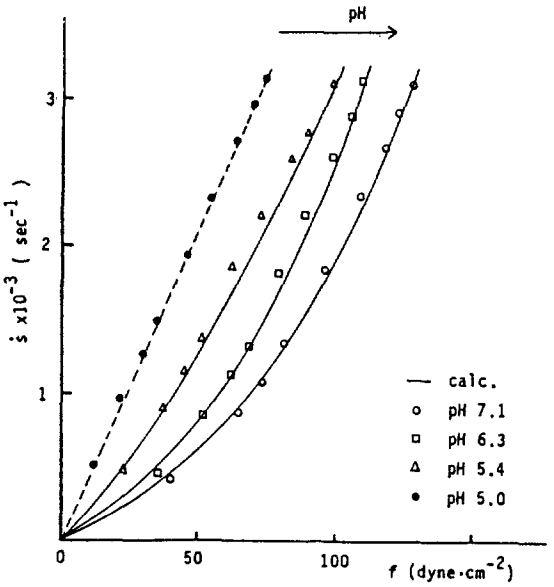


**Figure 4.** Flow curves of 35wt.% $TiO_2$(rutile)–water suspension with various pH at 25°C.

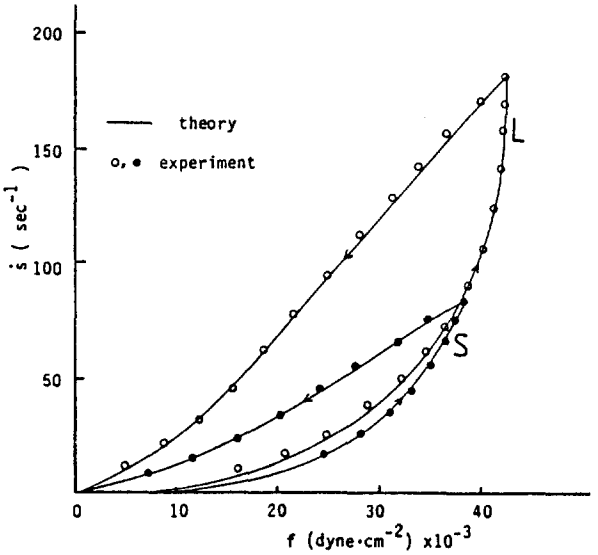


**Figure 5.** Hysteresis loops of "Second Down Oil Red Printing Ink"at 30°C. Curve L represents a large loop and S indicates a small one.

occurrs even in the course of the up-curve process.

**3. Printing Ink.** Up to now, we only treated the cases without hysteresis loop of the $TiO_2$–water system. Next, we consider the thixotropic system with hysteresis loops.

Green reported the thixotropic loops of printing ink, which were also analyzed by Hahn *et al.*[4] The experimental data shown in Figure 5 are those from the reference.[26]

We applied Eq.(9) and (11) to the up-curves and down-curves in Figure 5, respectively, and obtained the parametric values listed in Table 1. The theoretical curves in Figure 5 are the calculated ones from Eq. (9) and (11) by using the parametric data. The $\dot{s}_m$ values for the large and the small loops are 1100 and 170 sec$^{-1}$, respectively. We note a good agreement between theory and experiment.

[Note] In the application of Eq.(9) to the up-curve, it is assumed that $X_1$ is very large, $X_1+\Delta X_1 \cong X_1$, where $\Delta X_1$ is proportional to the flow units 1 detached from unit 2 in the course

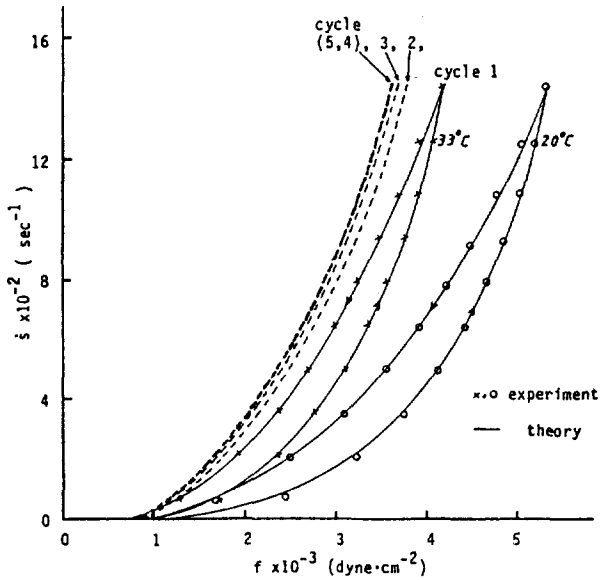


**Figure 6.** Hysteresis loops of mayonnaise at 20°C and 33°C. The curves 2 to 5 belong to the mayonnaise at 33°C, one notes that the hysteresis loops do not appear.

of the up-curve, and also that $\alpha_2$ is about constant irrespective of the detachment.

## Discussion

**1. Hysteresis Loop (Energy Loss).** The thixotropic loops in Figure 6 are those for the mayonnaise(Real Ribbon Mayonnaise, Knorr Korea LTD) at 20°C and 33°C. The loops were obtained by using a Couette-type rotational viscometer constructed in this laboratory. By applying Eq.(9) and (11), we obtained the parametric values in Table 1.

The character of the loops is following (1) the hysteresis loop shifts to the lower stress region at higher temperature, (2) the size of the higher temperature loop is smaller than that of the lower temmperature loop, and (3) the size of the thixotropic loops decreases with repeated cycling, eventually reaching a line curve. See Figure 6. This is due to the complete detachment of the small units from the unit 2 by the repeated cycling.

The area of the thixotropic loops represennt the energy loss during cyclic deformation. The area, built up by the up- and down-curves, is given by the double integral[27]

$$\text{Area}=\int_0^{\dot{s}_m}\int_{f_d(\dot{s})}^{f_u(\dot{s})} df\cdot ds \qquad (12)$$

Here, the first integral of d$f$ indicates the difference between the up-curve function $f_u(\dot{s})$ [Eq.(9)] and the down-curve function $f_d(\dot{s})$ [Eq.(11)]. Thus, Eq.(12) becomes, as,

$$\text{Area}=\int_0^{\dot{s}_m}[\sinh^{-1}\{(\beta_0)_2\dot{s}\cdot\exp(-c_2\dot{s}^2/RT)\} - \sinh^{-1}\{(\beta_0)_2\dot{s}\cdot\exp(-c_2\dot{s}_m^2/RT)\}]ds \qquad (12a)$$

In order to simplify the integration, we use the approximation

$$\sinh^{-1}x \cong \ln(2x) \quad (x \ll 1)$$

*i.e.*, $X=(\beta_0)_2\,\dot{s}\cdot\exp(-c_2\dot{s}^2/RT)>>1$ which is experimentally satisfied in practice. Then Eq.(12a) is simplified as follows:

**Table 2. Energy Losses(erg·cm$^{-3}$·sec$^{-1}$) in Cyclic Processes of the Mayonnaise System**

| Temperature (°C) | Energy loss calculated from Eq.(13) | Energy loss measured from the hysteresis loop |
|---|---|---|
| 20 | $5.639\times10^5$ | $5.955\times10^5$ |
| 33 | $4.203\times10^5$ | $4.591\times10^5$ |

$$\text{Area}=\frac{X_2}{\alpha_2}\int_0^{\dot{s}_m}\left(-\frac{c_2\dot{s}^2}{RT}+\frac{c_2\dot{s}_m^2}{RT}\right)d\dot{s}$$

$$=2/3\,(X_2/\alpha_2)\cdot(c_2/RT)\cdot\dot{s}_m^3 \qquad (13)$$

The area represented the energy loss per unit time and per unit volume (erg·cm$^{-3}$·sec$^{-1}$). Applying Eq.(13) to the mayonnaise system and by using the parametric values in Table 1, we calculated the area of hysteresis loop, results are shown in Table 2. By using a compensating planimeter, the area was directly measured, and the results are also shown in Table 2. One notes the agreement between the two results is very good.

**2. Relaxation Time.** In our equation, the parameters are determined by using the approximation $\sinh^{-1} x \cong \ln(2x)$ $(x>>1)$. This relation is applied to Eq.(10) and one obtains the following equation.

$$f=\frac{X_2}{\alpha_2}\ln[2(\beta_0)_2\exp(-c_2\dot{s}^2/RT)\cdot\dot{s}]$$

$$=\frac{X_2}{\alpha_2}[\ln(\beta_0)_2+\ln(2\dot{s})-c_2\dot{s}^2/RT] \qquad (14)$$

By apply Eq.(14) to an experimental flow curve of $TiO_2$ suspensions, the unkown parameters $X_2/\alpha_2$, $(\beta_0)_2$, and $c_2$/RT are obtained. In the cases with hysteresis loops, the parameters are obtained by the following procedures:

(1) by applying Eq.(11) to the down-curve, the parameters $X_0\beta_0/\alpha_0+X_1\beta_1/\alpha_1$, $X_2/\alpha_2$ and $(\beta_0)_2\cdot\exp(-c_2\dot{s}_m^2/RT)\equiv Z$ are obtained by using the approximation and solving the simultaneous equations; (2) by applying Eq.(9) to the up-curve, the $c_2/RT$ parameter is calculated; and (3) by multiplying $\exp(c_2\dot{s}_m^2/RT)$ value to $Z$, we obtain $(\beta_0)_2$.

Eu 28 obtained the same form of the Ree-Eyring equation in his paper "shear rate dependence of non-Newtoniann viscosity of fluids." He derived this equation from the Boltzmann equation and its dense fluid generalization under some resonable approximations. In his paper, the relaxation time, $\tau_e$, is unambiguously given in terms of Newtonian viscosity $\eta_0$, temperature $T$, density $n$ (numbers/volume), molecular diameter $d$ and the reduced mass $m_r$, *i.e.*,

$$\tau_e=2^{1/2}[\eta_0(2m_rkT)^{1/2}]^{1/2}/nkTd \qquad (15)$$

Therefore, if one knowns the Newtonian viscosity $\eta_0$ and molecular data, one can theoretically calculate the relaxation time $\tau_e$ from this relation. Our $(\beta_0)_2$ is the relaxation time for the flow units when there is no constraint. So, it is resonable to think that $(\beta_0)_2$ is the characteristic property of the system corresponding to $\tau_e$.

In order to compare the $\tau_e$ from Eq.(15) with the Ree-Eyring formula $(\beta_0)_2$, molecular diameter $d$ is changed into particle's diameter, $m_r$ and n are changed into the mass of a particle and the number of particles per unit volume, respectively. And the Newtonian viscosity $\eta_0$ in Eq.(15) was substituted by the term $\eta^{(N)}=X_0\beta_0\alpha_0+X_1\beta_1/\alpha_1$ which is obtained from Eq.(9), since Eu's $\eta_0$ is the rare gases viscosity which cannot be used in the comparison. The term $\eta^{(N)}$ in Eq.(9) was neglected compared to the non-Newtonian term in the calculation of the $TiO_2$ curve. However the size of $\eta^{(N)}$ is calculable, thus the calculated $\eta^{(N)}$ was used in the comparison. The comparison of the relaxation times are shown in Tale 3, where a good agreement between $(\beta_0)_2$ and $\tau_e$ is noted.

**Table 3. Relaxation times $(\beta_0)_2$ of the $TiO_2$-Water System from Eq.(10) and Those $(\tau_e)$ Calculated from Eu's Theory [Eq.(15)]**

| $TiO_2$ Types | pH | $\eta_0^{(N)}$ (N·sec/m$^2$) from Eq.(9) | $(\beta_0)_2\times10^3$ (sec) | $\tau_e\times10^3$ (sec) |
|---|---|---|---|---|
| Anatase | | | | |
| $d=0.3\mu^a$ | 3.6 | $1.04\times10^{-2}$ | 16.4 | 12.2 |
| $m_r=5.18\times10^{-17}$kg$^b$ | 4.4 | $3.97\times10^{-3}$ | 9.55 | 7.56 |
| $n=7.72\times10^{16}$/m$^{3c}$ | 5.7 | $2.48\times10^{-3}$ | 2.45 | 5.98 |
| Rutile | | | | |
| $d=0.2\mu^a$ | 5.4 | $3.84\times10^{-4}$ | 0.75 | 0.74 |
| $m_r=1.70\times10^{-17}$kg$^b$ | 6.3 | $6.51\times10^{-4}$ | 1.73 | 0.95 |
| $n=2.82\times10^{19}$/m$^{3c}$ | 7.1 | $8.26\times10^{-4}$ | 2.07 | 1.08 |

[a]The particle size in our system was $\sim\mu$. [b]The density of the $TiO_2$(anatase)$=3.84\times10^3$ kg/m$^3$. The density of the $TiO_2$(rutile)$=4.26\times10^3$kg/m$^3$. From the densities, the $m_r$ values were estimated. [c]The anatase: 45g in 115 cm$^3$ of 30wt.% suspension, the rutile: 55g in 115 cm$^3$ of 35wt.% suspension. From these data, the n values were estimated.

**3. Reconsideration of the Model of Flow Unit 2.** Here we consider why the model presented in Figure 1 can express the thixotropic systems. In the $TiO_2$-suspension systems, the $TiO_2$ fine-particles are connected with each other, and make a tiny cluster having some inelasticity. The main spring in Figure 1 corresponds to this $TiO_2$-cluster in the suspension, and the micro $TiO_2$-fragments correspond to the small springs in Figure 1 acting as flow unit 1.

Printing ink is a system of pigments(organic or inorganic) suspended in vehicles(oils). The pigments behave just like the $TiO_2$ in the abovementioned suspension. In this case, however, the reattachment of the detached micro-groups to the cluster is not fast, thus hysteresis loop appears.

Mayonnaise is an emulsion system, vegetable oils emulsified by egg yolk. The protein molecule acts as a chain(unit 2) to which oil droplets(unit 1) attach. The oil droplets can be detached completely by repeated cycling. Thus, hysteresis loop becomes smaller with repeated cycling, eventually it disappears.

## References

1. H.A. Mercer and H.D. Weymann, *Trans. Soc. Rheol.*, **1**, 199 (1974).
2. J. Mewis and R. de Bleyser, *J. Colloid Interface Sci.*, **40**, 360 (1972).
3. W.H. Bauer and E.A. Collins, "Rheology; Theory and Applications," in F.R. Eirich (Ed.), Academic Press, New York, 1967, Vol. 4, pp. 423-459.
4. S.J. Hahn, T. Ree and H. Eyring, (a) *Ind. Eng. Chem.*,

**51,** 856 (1959); (b) NLGI Spokesman (Jour. Natl. Lubricating Grease Inst., **23,** 129 (1959)
5. G.B. Thurston, *Biorheology,* **16,** 149 (1979).
6. R. Giordano, M.P. Fontana and F. Wanderlingh, *J. Chem. Phys.,* **74,** 2011 (1981).
7. R. Lapasin, V. Longo and S. Rajgelj, in "Rheology(Proc. VIIIth International Congress on Rheology, Naples, 1980), "[G. Astarita, G. Marrucci and L. Nicolais (Ed.)], Plenum Press(N.Y. 1980), Vol. 3, pp. 659-664.
8. R. Lapasin, A. Papo and S. Rajgelj, *Rheol. Acta,* **22,** 410(1983).
9. J. Mewis, *J. Non-Newtonian Fluid Mech.,* **6,** 1 (1979).
10. D.D. Joye and G.W. Poehlein, *Trans. Soc. Rheol.,* **15,** 51 (1971).
11. J. Mewis, A.J.B. Spaull and J. Helsen, *Nature,* **253,** 618 (1975).
12. R.A. Ritter and G.W. Govier, *Canad. J.Ch.E.,* **48,** 505 (1970).
13. V.V. Chavan, A.K. Deysarkar and J. Ulbrecht, *Chem. Eng. J.,* **10,** 205 (1975).
14. S. Glasstone, K.J. Laidler and H. Eyring, "The Theory of Rate Processes," McGraw-Hill, New York and London, 1941, pp. 477-551.
15. T. Ree and H. Eyring, *J. Appl. Phys.,* **26,** 793, 800 (1955).
16. S.J. Hahn, T. Ree and H. Eyring, NLGI Spokesmman (the Journal of the National Lubricating Grease Institute), **21,** 12 (1957).
17. I.M. Krieger and T.J. Dougherty, *Trans. Soc. Rheol.,* **3,** 137 (1959).
18. D.C-H. Cheng and F. Evans, *Brit. J. Appl. Phys.,* **16,** 1599 (1965).
19. D.C-H. Cheng, *Brit. J. Appl. Phys.,* **17,** 253 (1966).
20. A.G. Fredrickson, *A.I.Ch.E.J.,* **16,** 436 (1970).
21. K. Park and T. Ree, *J. Korean Chem. Soc.,* **15,** 293 (1971).
22. H. Utsugi and T. Ree, *Advances Chem. Phys.,* **21,** 273 (1971).
23. A. Einstein, *Ann. Physik,* **19,** 289 (1906), L.D. Landau and E.M. Lifshitz, "Fluid Mechanics," Pergamon, London, 1959, p. 76.
24. J.H. Bang, E.R. Kim, S.J. Hahn and T. Ree, *Bull. Korean Chem. Soc.,* **4,** 212 (1983).
25. C.W. Lee, E.R. Kim and S.J. Hahn, *Journal of the Research Institute of Industrial Sciences, Hanyang University,* **21,** 253 (1985).
26. H. Green, "Industrial Rheology and Rheological Strutures," John Wiley, New York, 1949, p. 133.
27. E. Kreyszig, "Advanced Engineering Mathematics" (5th), John Wiley and Sons, New York, 1983, p. 414.
28. B.C. Eu, *J. Chem. Phys.,* **79,** 2315 (1983).

# Test of a Multi-Reference Many-Body Perturbation Theory for the Description of Electron Correlations in four Valence Electron States of Transition Metal Atoms

**Yoon Sup Lee*, Hosung Sun†, Karl F. Freed‡, and S. Hagstrom§**

**Department of Chemistry, Korea Advanced Institute of Science and Technology Seoul, 131*

†*Department of Chemistry, Pusan National University, Pusan 607*

‡*The James Franck Institute and Department of Chemistry, The University of Chicago, Chicago, Illinois 60637 U.S.A.*

§*Department of Chemistry, Indiana University, Bloomington, Indiana 47405, U.S.A.*

*Received March 3, 1986*

A multi-reference many-body perturbation theory (MRMBPT) method is critically tested in second order by comparing with the corresponding configuration interaction (CI) calculations. Excitation energies of the four-valuence-electron states of transition metal atoms and ions are used for the comparison. The agreement between the second order MRMBPT and CI calculations is very reasonable, confirming the reliability of the second order MRMBPT method. The reliability of calculations with the present second order MRMBPT method was only been inferred empirically in the past since most results have been gauged by the agreement with experiment and/or with other MRMBPT calculations based upon different sets of orbitals and configuration spaces. The present MRMBPT method appears to be an efficient ab initio multi-reference method for the calculation of electron correlation effects in atoms and molecules, and it is shown how MRMBPT can be used to estimate core-core and core-valence correlation effects which are often omitted in CI calculations because too many configurations and correlating electrons are involved.

## Introduction

Many-body perturbation theory (MBPT) is one of the common techniques for the study of electron correlation, an effect which is important for the accurate description of the electronic structure of atoms and molecules. The conventional